

# Synthesis and Properties of a (Diarylamino)ferrocene and Its Radical Cation

Arjun Mendiratta,<sup>†</sup> Stephen Barlow,<sup>\*,†,‡</sup> Michael W. Day,<sup>†</sup> and Seth R. Marder<sup>†,§,⊥</sup>

Beckman Institute, 139-74, California Institute of Technology, Pasadena, California 91125, Jet Propulsion Laboratory, California Institute of Technology, Pasadena, California 91109, and Department of Chemistry, University of Arizona, Tucson, Arizona 85721

Received August 31, 1998

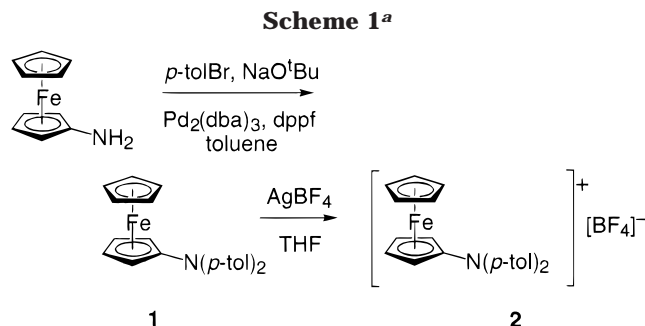
**Summary:** (Di-*p*-tolylamino)ferrocene (**1**) was synthesized using Pd-catalyzed C–N bond formation; it is oxidized at –250 mV vs ferrocene in THF. Magnetic susceptibility measurements show the unpaired electron of [1]<sup>+</sup>[BF<sub>4</sub>]<sup>–</sup> (**2**) to be principally ferrocene-localized; however, the diarylamino moiety leads to a substantial red shift of the ligand-to-metal charge-transfer transition of **2** relative to that of ferrocenium.

## Introduction

“Electron-rich”, i.e., low oxidation potential, ferrocenes have been studied as components of magnetic materials,<sup>1</sup> as electrode surface modifiers,<sup>2</sup> and as nonlinear optical chromophores.<sup>3</sup> While most work has focused on penta-, octa-, and nonamethylated derivatives,<sup>4</sup> aminoferrocene derivatives represent an alternative, little-explored class of “electron-rich” ferrocenes. Previous routes to (diarylamino)ferrocenes have been based upon Ullmann-type couplings of bromoferrocene and diarylamide anions.<sup>5</sup> Ullmann couplings are notoriously variable in yield, and the efficient synthesis of bromoferrocene requires the handling of environmentally hazardous chloromercurioferrocene.<sup>6</sup> Therefore, we were interested in developing an alternative route to (diarylamino)ferrocenes. Here we describe the application of recently reported Pd-catalyzed diaryl- and triarylamine syntheses<sup>7,8</sup> to the preparation of (di-*p*-tolylamino)ferrocene (**1**). The properties and crystal structure of **1** and the properties of its one-electron-oxidation product (**2**) are also described.

## Results and Discussion

The Pd-catalyzed coupling of aminoferrocene and excess *p*-bromotoluene (Scheme 1) under rigorously



<sup>a</sup> Legend: dba = dibenzylideneacetone, dppf = 1,1'-bis-(diphenylphosphino)ferrocene.

deoxygenated conditions gave **1** in a yield (58%) similar to that reported for the Ullmann-type procedure for (diphenylamino)ferrocene (67%).<sup>5</sup> In the presence of oxygen, azoferrocene was found to be the major isolable product; the oxidation of aminoferrocene to azoferrocene under different conditions has previously been reported.<sup>5</sup> Attempts to couple bromoferrocene and *p*-tolylamine were unsuccessful; these results are consistent with previous studies of electron-rich aryl bromides.<sup>7,8</sup> Thus, the Pd-catalysis route to (diarylamino)ferrocenes is complementary to the traditional Ullmann route in that the ferrocene source is aminoferrocene (a convenient synthesis of which has recently been published<sup>9</sup>) rather than bromoferrocene. The avoidance of bromoferrocene also has the advantage of circumventing the mercury chemistry used to synthesize bromoferrocene.

Compound **1** has been characterized by elemental analysis, <sup>1</sup>H and <sup>13</sup>C NMR spectroscopy, and UV–vis spectroscopy; the UV–vis spectrum is essentially identical with the published spectrum of (diphenylamino)ferrocene.<sup>10</sup> We also determined the crystal structure of **1**. A view of one of the two independent molecules in the asymmetric unit is shown in Figure 1; bond lengths and angles are given in the Supporting Information.

The electrochemistry of **1**, together with that of two other ferrocenyl nitrogen compounds, is summarized in Table 1. Figure 2 shows the cyclic voltammogram of **1**. Clearly **1** is considerably more susceptible to oxidation than ferrocene; for comparison, we measured the potential of the [Fe(C<sub>5</sub>Me<sub>4</sub>H)<sub>2</sub>]<sup>+</sup>/Fe(C<sub>5</sub>Me<sub>4</sub>H)<sub>2</sub> couple to be –360 mV vs ferrocenium/ferrocene in THF (–445 mV

<sup>†</sup> Beckman Institute, California Institute of Technology.

<sup>‡</sup> Present address: Inorganic Chemistry Laboratory, University of Oxford, South Parks Road, Oxford, OX1 3QR, U.K.

<sup>§</sup> Jet Propulsion Laboratory, California Institute of Technology.

<sup>⊥</sup> University of Arizona.

(1) Miller, J. S.; Epstein, A. J. *Angew. Chem., Int. Ed. Engl.* **1994**, *33*, 385–415 and references therein.

(2) Zou, C.; Wrighton, M. S. *J. Am. Chem. Soc.* **1990**, *112*, 7578–7584.

(3) Barlow, S.; Bunting, H. E.; Ringham, C.; Green, J. C.; Bublitz, G. U.; Boxer, S. G.; Perry, J. W.; Marder, S. R. Submitted for publication.

(4) Hradsky, A.; Bildstein, B.; Schuler, N.; Schottenberger, H.; Jaitner, P.; Ongania, K.-H.; Wurst, K.; Launay, J.-P. *Organometallics* **1997**, *16*, 392–402 and references therein.

(5) Nesmeyanov, A. N.; Sazonova, V. A.; Romanenko, V. I. *Dokl. Akad. Nauk SSSR* **1964**, *157*, 922–925.

(6) Fish, R. W.; Rosenblum, M. *J. Org. Chem.* **1965**, *30*, 1253–11254.

(7) Hartwig, J. F. *Angew. Chem., Int. Ed. Engl.* **1998**, *37*, 2046–2066 and references therein.

(8) Thayumanavan, S.; Barlow, S.; Marder, S. R. *Chem. Mater.* **1997**, *9*, 3231–3236.

(9) Montserrat, N.; Parkins, A. W.; Tomkins, A. R. *J. Chem. Res., Synop.* **1995**, 336–337.

(10) Herberhold, M.; Ellinger, M.; Kremnitz, W. *J. Organomet. Chem.* **1983**, *241*, 227–240.

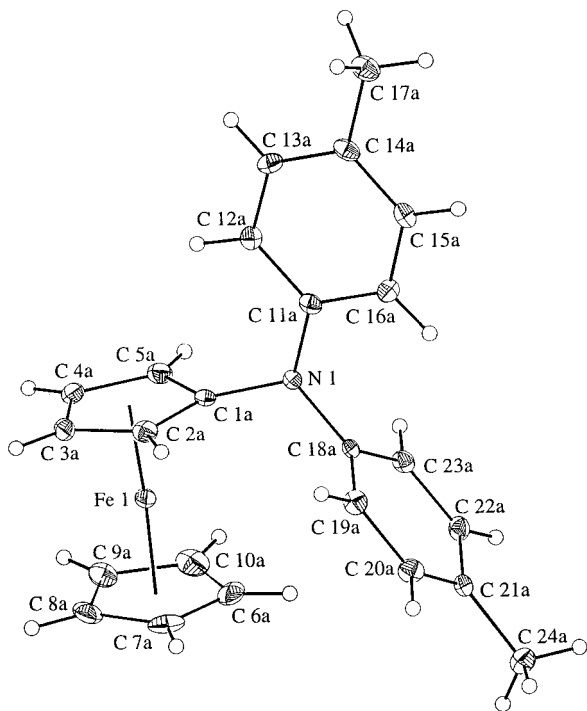


**Figure 1.** View of one of the two independent molecules of **1** in the crystal structure. Non-hydrogen atoms are represented by 50% probability ellipsoids.

**Table 1. Half-Wave Potentials for Three Nitrogen-Substituted Ferrocene Derivatives, Measured Using Cyclic Voltammetry in THF and CH<sub>2</sub>Cl<sub>2</sub> (0.1 M [nBu<sub>4</sub>N]<sup>+</sup>[PF<sub>6</sub>]<sup>-</sup>) at a Scan Rate of 50 mV s<sup>-1</sup> (Fc = Ferrocenyl)**

compd	THF		CH <sub>2</sub> Cl <sub>2</sub>	
	$E_{1/2}(1)^a/\text{mV}$	$E_{1/2}(2)^a/\text{mV}$	$E_{1/2}(1)^a/\text{mV}$	$E_{1/2}(2)^a/\text{mV}$
<b>1</b>	-255	$E_{\text{ox}} = +715^b$	-285	<i>c</i>
FcNH <sub>2</sub>	-405	$E_{\text{ox}} = +660^b$	-350	<i>c</i>
FcN=NFc	+110	+280	+95	+330

<sup>a</sup>  $E_{1/2}(1)$  and  $E_{1/2}(2)$  are half-wave potentials vs ferrocenium/ferrocene for the [m]<sup>+</sup>/[m] and [m]<sup>2+</sup>/[m]<sup>+</sup> couples, respectively. <sup>b</sup> Irreversible; peak potentials given. <sup>c</sup> Not observable within solvent window.

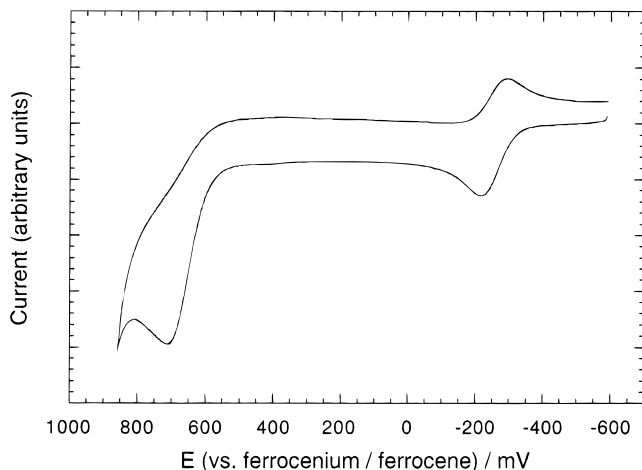


**Figure 2.** Cyclic voltammogram of **1** recorded in THF (0.1 M [nBu<sub>4</sub>N]<sup>+</sup>[PF<sub>6</sub>]<sup>-</sup>) at a scan rate of 50 mV s<sup>-1</sup>.

vs ferrocenium/ferrocene in dichloromethane). Aminoferrocene is even more readily oxidized than **1**; presumably the nitrogen lone pair of FcNH<sub>2</sub> can act as a more effective donor in this species, whereas in **1** conjugation

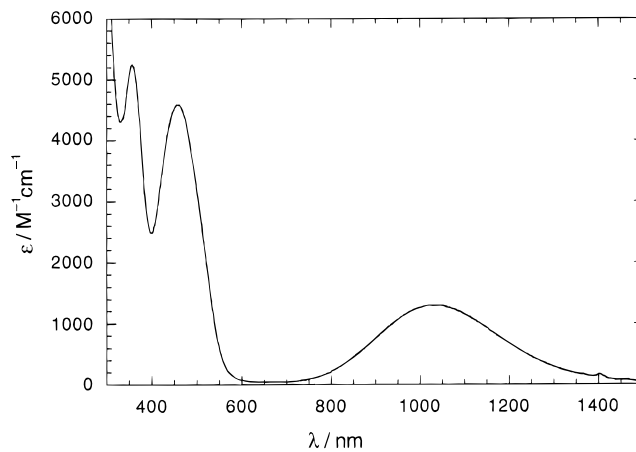


**Figure 3.** UV-vis-near-IR spectrum of **2** in dichloromethane.

is reduced due to twisting of the ferrocenyl group arising from the steric demands of the tolyl groups (see Figure 1). In THF irreversible second oxidations at higher potential are seen for both [**1**]<sup>+</sup> and the aminoferrocene cation.<sup>11</sup> Azoferrocene shows two reversible redox processes, attributable to successive oxidation of the two ferrocene centers. The separations between the two redox processes,  $\Delta E_{1/2} = E_{1/2}(2) - E_{1/2}(1)$ , are 190 and 235 mV in THF and dichloromethane, respectively. Interestingly, *trans*-FcCH=CHF<sub>c</sub> is reported to show  $\Delta E_{1/2}$  values of 0 and 140 mV in the same two solvents,<sup>12</sup> suggesting a weaker metal-metal interaction in the carbon-bridged species; however, this conclusion is at variance with that indicated by interaction parameters deduced from the intervalence charge-transfer absorptions of [FcN=NFc]<sup>+</sup> and [FcCH=CHF<sub>c</sub>]<sup>+</sup>.<sup>13</sup>

We chemically oxidized **1** to its tetrafluoroborate salt, **2**, using AgBF<sub>4</sub>. The temperature dependence of the magnetic susceptibility of **2** obeys the Curie-Weiss law with a Curie constant of 0.546 emu K mol<sup>-1</sup> and a Weiss constant of -0.32 K. The effective room-temperature magnetic moment of 2.1 μ<sub>B</sub> is consistent with an  $S = 1/2$  cation with an average  $g$  value ( $\langle g \rangle$ ) of 2.4. This indicates that the positive charge is principally ferrocene-based; values of  $\langle g \rangle$  for ferrocenium ions range between ca. 2.3 and ca. 2.8,<sup>14-17</sup> while an isotropic  $g$  tensor of ca. 2.00 is anticipated for amine-centered radical cations.<sup>18</sup> The UV-vis-near-IR spectrum of **2** is shown in Figure 3. The lowest energy absorption maximum occurs at 1026 nm in dichloromethane (983 nm in acetonitrile). This maximum is considerably red-shifted from that of the unsubstituted ferrocenium ion (745 nm in acetonitrile);<sup>19</sup>

(11) For comparison, we measured the oxidation of triphenylamine under the same conditions and found  $E_{\text{ox}} = +655$  mV vs ferrocenium/ferrocene.

(12) Floris, B.; Tagliatesta, P. *J. Chem. Res., Synop.* **1993**, 42-43.

(13) Delgado-Peña, F.; Talham, D. R.; Cowan, D. O. *J. Organomet. Chem.* **1983**, 253, C43-C46.

(14) Prins, R.; Korswagen, A. R. *J. Organomet. Chem.* **1970**, 25, C74-C76.

(15) Prins, R. *Mol. Phys.* **1970**, 19, 603-620.

(16) Duggan, D. M.; Hendrickson, D. N. *Inorg. Chem.* **1975**, 14, 955-969.

(17) O'Hare, D.; Green, J. C.; Marder, T.; Collins, S.; Stringer, G.; Kakkar, A. K.; Kaltsoyannis, N.; Kuhn, A.; Lewis, R.; Mehnert, C.; Scott, P.; Kurmoo, M.; Pugh, S. *Organometallics* **1992**, 11, 48-55.

(18) Neugebauer, F. A.; Bamberger, S.; Groh, W. R. *Chem. Ber.* **1975**, 108, 2406-2415.

(19) Toma, S.; Gáplovsky, A.; Hudeček, M.; Langfelderová, Z. *Monatsh. Chem.* **1985**, 116, 357-364.

similar red shifts have been noted for arylferrocenium ions with electron-donating groups in the para position.<sup>19</sup> These observations are consistent with the assignment of the low-energy band of the ferrocenium ion as a ligand–metal charge transfer.<sup>20</sup>

### Experimental Details

Elemental analyses were performed by Atlantic Microlab Inc., Norcross, GA. FT NMR spectra were recorded using a General Electric QE-300 spectrometer. UV–vis–near-IR spectra were acquired using a Varian Cary 5E spectrometer. Cyclic voltammetry was performed under argon on tetrahydrofuran or dichloromethane solutions ca.  $10^{-4}$  M in sample and 0.1 M in [<sup>n</sup>Bu<sub>4</sub>N]<sup>+</sup>[PF<sub>6</sub>]<sup>−</sup> using a glassy-carbon working electrode, a platinum auxiliary electrode, a AgCl/Ag pseudo-reference electrode, and a BAS 100B potentiostat. Potentials were referenced by the addition of ferrocene to the cell and are quoted to the nearest 5 mV relative to the ferrocenium/ferrocene couple at 0 V. SQUID magnetic susceptibility data were acquired as described elsewhere.<sup>21</sup> THF and diethyl ether were distilled from sodium benzophenone ketyl; toluene and dichloromethane were distilled from calcium hydride. Bromoferrocene<sup>6</sup> and aminoferrocene<sup>9</sup> were prepared by literature procedures; all other reagents were obtained from commercial sources and used without further purification.

**(Di-*p*-tolylamino)ferrocene (1).** A mixture of tris(dibenzylideneacetone)dipalladium, Pd<sub>2</sub>(dba)<sub>3</sub> (139.7 mg, 0.150 mmol), and 1,1'-bis(diphenylphosphino)ferrocene, dppf (130 mg, 0.234 mmol), in toluene (20 mL) was stirred under nitrogen for 10 min. Sodium *tert*-butoxide (719 mg, 7.5 mmol) and *p*-bromotoluene (1.54 g, 9 mmol) were then added, and the mixture was stirred for an additional 10 min. A solution of aminoferrocene (620 mg, 3.1 mmol) in toluene (10 mL) was then added, and the resulting mixture was freeze–pump–thaw degassed. The sealed reaction vessel was then heated to 90 °C for 72 h. The mixture was then cooled to room temperature, poured into water, and extracted with diethyl ether until the extracts were colorless. The combined organic extracts were dried over magnesium sulfate and filtered before solvent removal under reduced pressure. The crude product was purified by flash chromatography on silica gel, with toluene/hexane (1:1) as eluent, to give pure **1** (665 mg, 58%). Orange-red crystals suitable for X-ray crystallography were grown from hexanes. <sup>1</sup>H NMR (300 MHz, chloroform-*d*): δ 7.15 (d, *J* = 8.5 Hz, 4H), 7.10 (d, *J* = 8.5 Hz, 4H), 4.16 (s, 5H), 3.99 (apparent s, 4H), 2.32 (s, 6H). <sup>13</sup>C NMR (75 MHz, chloroform-*d*): δ 145.2, 132.4, 129.6, 124.5, 108.0, 68.8, 63.6, 59.1, 20.8; UV–vis (hexanes): λ<sub>max</sub> 252 (ε<sub>252</sub> 9000), 291 (ε<sub>291</sub> 10 000), 454 (ε<sub>454</sub> 300) nm (M<sup>−1</sup> cm<sup>−1</sup>). Anal. Calcd for C<sub>24</sub>H<sub>23</sub>NFe: C, 75.6; H, 6.08; N, 3.67. Found: C, 75.9; H, 6.20; N, 3.75. *Note!* The reaction mixture must be rigorously deoxygenated before heating; in other attempts to synthesize **1**, the presence of oxygen led to the formation of azoferrocene, FcN=NFc, under the reaction conditions. The azoferrocene was isolated after flash chromatography on silica gel (5:1 hexane/EtOAc) and identified by its UV–vis spectrum.<sup>22,23</sup>

(20) Sohn, Y. S.; Hendrickson, D. N.; Gray, H. B. *J. Am. Chem. Soc.* **1971**, *93*, 3603–3612.

(21) Murray, M. M.; Kaszynski, P.; Kaisaki, D. A.; Chang, W. H.; Dougherty, D. A. *J. Am. Chem. Soc.* **1994**, *116*, 8152–8161.

(22) Nesmeyanov, A. N.; Perevalova, E. G.; Nikitina, T. V. *Tetrahedron Lett.* **1960**, 1–2.

(23) Nesmeyanov, A. N.; Perevalova, E. G.; Nikitina, T. V. *Dokl. Akad. Nauk SSSR* **1961**, *138*, 1118–1121.

**(Di-*p*-tolylamino)ferrocenium Tetrafluoroborate (2).** All manipulations were performed under a nitrogen atmosphere. To a solution of **1** (169 mg, 0.44 mmol) in THF (10 mL) was added dropwise a solution of silver tetrafluoroborate (77.6 mg, 0.40 mmol) in THF (10 mL). The resulting mixture was stirred for 18 h. The solvent was evaporated under reduced pressure, and the resulting solid was washed three times with diethyl ether (3 × 25 mL) and extracted into dichloromethane (ca. 50 mL). The dichloromethane extracts were filtered through Celite and evaporated under reduced pressure to yield a dark orange powder. Analytically pure crystals were grown by layering a concentrated dichloromethane solution with diethyl ether. The solvent was decanted from the resulting dark orange, slightly air-sensitive, needles, which were then washed three times with diethyl ether and dried in vacuo (102 mg, 0.22 mmol, 50%). UV–vis–near-IR (CH<sub>2</sub>Cl<sub>2</sub>): λ<sub>max</sub> 356 (ε<sub>356</sub> 5300), 458 (ε<sub>458</sub> 4700), 1027 (ε<sub>1027</sub> 1300) nm (M<sup>−1</sup> cm<sup>−1</sup>). UV–vis–near-IR (THF): λ<sub>max</sub> 352, 450, 981 nm. UV–vis–near-IR (CH<sub>3</sub>CN): λ<sub>max</sub> 351, 448, 983 nm. <sup>1</sup>H NMR (300 MHz, dichloromethane-*d*<sub>2</sub>): δ 21.1, 13.1, 9.8, 1.6–0.4 (broad), −10.1. Anal. Calcd for C<sub>24</sub>H<sub>23</sub>NFeBF<sub>4</sub>: C, 61.6; H, 4.95; N, 2.99. Found: C, 61.4; H, 4.99; N, 3.07.

**X-ray Structure Determination of 1.** A golden yellow lozenge (0.41 × 0.37 × 0.37 mm) of C<sub>24</sub>H<sub>23</sub>FeN (FW = 381.28) belonged to the monoclinic space group *P*2<sub>1</sub>/*c* with *a* = 14.311(4) Å, *b* = 12.926(3) Å, *c* = 19.656(5) Å, β = 92.19(2)°, *V* = 3633.4(16) Å<sup>3</sup>, *Z* = 8 (i.e. two independent molecules in the asymmetric unit), and μ = 0.837 mm<sup>−1</sup>. A total of 16 775 (6381 independent) reflections were measured over the range 1.9–25.0° at 85 K using an Enraf Nonius CAD-4 diffractometer. No absorption correction was applied to the data. The structure was solved using SHELXS-97<sup>24</sup> and refined using SHELXL-97; all non-hydrogen atoms were revealed by the direct-methods solution, while hydrogen atoms were located using difference Fourier maps. Full refinement (positional and anisotropic displacement parameters of non-hydrogen atoms, positional and isotropic displacement parameters of hydrogen atoms) on *F*<sup>2</sup>, against *all* reflections, converged with *R*1 = 0.0282 and *wR*2 = 0.0602 for *I* > 2σ(*I*) (*R*1 = 0.0352 and *wR*2 = 0.0619 for all data). Full details are given in the Supporting Information.

**Acknowledgment.** Support from the National Science Foundation, Air Force Office of Scientific Research (AFOSR), at Caltech is gratefully acknowledged. The research described in this paper was performed in part by the Jet Propulsion Laboratory (JPL), California Institute of Technology, as part of its Center for Space Microelectronics Technology and was supported by the Ballistic Missile Defense Initiative Organization, Innovative Science and Technology Office, through an agreement with the National Aeronautics and Space Administration (NASA). We also thank Dr. Seth Miller for valuable assistance with the SQUID measurements.

**Supporting Information Available:** Tables of crystal structure solution and refinement details, atomic coordinates and equivalent isotropic displacement parameters, bond lengths and angles, anisotropic displacement parameters, and hydrogen coordinates and isotropic displacement parameters for **1**. This material is available free of charge via the Internet at <http://pubs.acs.org>.

OM980733G

(24) Sheldrick, G. M. *Acta Crystallogr.* **1990**, *A46*, 467–473.